IOP Publishing Journal of Micromechanics and Microengineering
J. Micromech. Microeng. **17** (2007) 994–1001 doi:10.1088/0960-1317/17/5/020

Biocompatible coatings for CMUTs in a harsh, aqueous environment

X Zhuang[1,3], A Nikoozadeh[1,3], M A Beasley[1,3], G G Yaralioglu[1], B T Khuri-Yakub[1] and B L Pruitt[2]

[1] Department of Electrical Engineering, Stanford University, Stanford, CA, USA
[2] Department of Mechanical Engineering, Stanford University, Stanford, CA, USA

Received 21 October 2006, in final form 23 March 2007
Published 17 April 2007
Online at stacks.iop.org/JMM/17/994

Abstract
The results of coating capacitive micromachined ultrasonic transducer (CMUT) arrays with two different biocompatible materials, parylene-c and polydimethylsiloxane (PDMS), are reported. These materials were characterized for use with CMUTs to enable direct contact transcutaneous and *in vivo* imaging. A passivation coating is required to provide electrical isolation to the active areas of the device and to protect it from a corrosive environment. It must also provide good mechanical characteristics to void imaging artifacts. The coated devices were compared side by side with uncoated devices for testing in air. The resonant frequency, collapse voltage and crosstalk were sampled. Parylene coated CMUTs were also tested underwater using pulse excitation. The parylene coating provided electrical insulation to the aqueous solution for 14 days. Both coatings showed a decrease in device resonant frequency and an increase in collapse voltage, as expected from the proposed theory.

(Some figures in this article are in colour only in the electronic version)

1. Introduction

Current ultrasound imaging devices include composite and non-composite piezoelectric transducers that require high precision, labor-intensive mechanical dicing and lapping. As higher frequencies are being sought for ultrasound that would allow greater image resolution for applications such as small animal imaging, piezoelectric transducers are being scaled to smaller dimensions that require additional fabrication complexity. The capacitive micromachined ultrasonic transducer (CMUT) is a new transducer technology under intense research. It has been demonstrated as a promising technology for ultrasonic imaging [1–4]. CMUTs are made with batch fabrication techniques employed by the semiconductor industry, which is much more versatile than the mechanical dicing method for fabricating piezoelectric transducers, and are readily scalable in size. Additionally, the CMUT fabrication method allows multiplexing, pulsing and pre-amplifying electronics to be easily integrated on the same chip with the transducers or on a separate chip via flip-chip bonding. This allows for 1D and 2D arrays of elements to be easily steered electronically, versus one mechanically steered piezoelectric transducer. CMUTs offer low unit cost, wide bandwidth and broad operation frequency range. A CMUT comprises a number of membranes over vacuum cavities. The membranes are deflected electrostatically and actuated in ac bursts to generate ultrasonic waves into the medium. Acoustic waves impinging on the membranes causes capacitance change, which is sensed by external circuitry. Figure 1 shows a cross section of two CMUT cells connected in parallel.

In order to use CMUTs in contact with living tissue or inside the living animals, a biocompatible material must coat the device and provide electrical isolation to the active areas of each array element. With membrane dc bias voltages ranging up to 200 volts, a coating is also necessary to protect living tissue from these high voltages. The coating must be thin to mitigate effects on device performance, but at the same time thick enough to prevent dielectric breakdown. In summary, CMUTs require a biocompatible passivation material that can be conformal for full coverage, electrically insulating, thin to reduce composite damping, impermeable to moisture and gases, and thermally and mechanically stable. Similar work has been done in this area for piezoelectric transducers.

[3] These authors contributed equally to the manuscript.

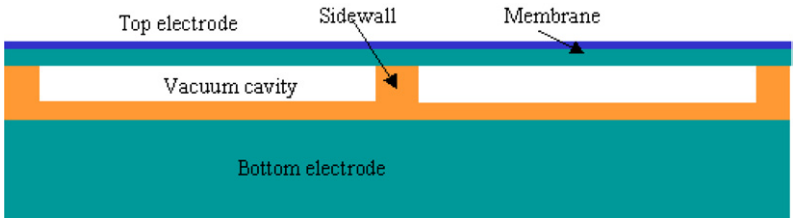

Figure 1. Cross section of two CMUT cells connected in parallel.

Table 1. Mechanical properties of coatings, device membrane and water.

	Parylene-c	PDMS	Silicon	Water
Young's modulus (MPa)	2700 [5]	0.5–1 [6]	168 000	–
Poisson's ratio	~0.4 [7]	0.5 [8]	0.17	~0.5
Density (kg m^{-3})	1289 [5]	970 [8]	2330	1000
Dielectric breakdown (V μm^{-1})	220 [5]	~14	–	–
Sound velocity (m s^{-1})	2202	~1200	8433	1540
Acoustic impedance (MRayl)	2.84	1.16	19.65	1.54

However, for piezoelectric transducers impedance matching to the surrounding medium is a big issue. Usually a protective coating for these transducers is applied on top of the thick (of the order of a quarter wavelength) impedance matching layers [9–11]. For CMUTs, on the other hand, impedance matching is not a problem due to the very low acoustic impedance of membranes. This allows for the coating for biocompatibility to be directly applied on the membrane.

Many materials have been evaluated for biocompatibility, including many already common to silicon micromachining. Silicon, silicon dioxide, silicon nitride, silicon carbide, metallic gold and polymers such as SU-8 photoresist, parylene, PDMS and polyimide exhibit reasonable biocompatibility [12–14]. For this study, parylene and PDMS were chosen for their key material properties. These materials are widely used and available. Their coating techniques are relatively low cost and compatible with MEMS. Parylene has been shown to provide reliable passivation schemes for MEMS underwater sensors [15, 16]. PDMS was also used in this study to determine the effects of a softer coating. Table 1 summarizes the key material properties for these two coating materials, as well as those of the silicon membrane and water.

2. Device modeling and effect of coating

A CMUT can be modeled as a simple capacitor formed between two electrodes separated by a vacuum gap. The dc voltage applied between the top and bottom electrodes generates an electrostatic force that causes the membrane to deflect. If the dc bias is less than the collapse voltage, the electrostatic force and the mechanical restoring force exerted by the membrane counterbalance each other. In the transmit mode, an ac voltage, on top of the dc bias, is applied to generate ultrasound waves in the surrounding medium. In the receive mode, the incoming ultrasound wave causes the membrane to vibrate, and is detected by the change in capacitance.

An in-house software package has been developed at Stanford University to simulate the behavior of CMUT under numerous static and dynamic conditions. The core of this program relies on accurate calculation of displacement profile

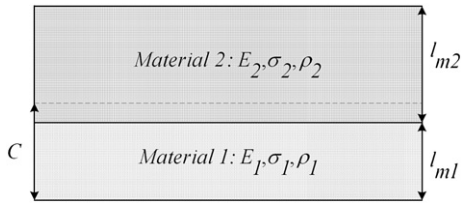

Figure 2. A schematic of a compound plate composed of two different materials.

of the membrane for a specific dc bias voltage [17]. In summary, this program uses the governing equation of motion of a plate that, in a simple form, can be written as

$$D\nabla^4 w = P. \tag{1}$$

In this equation, D is the flexural rigidity of the plate, w is the displacement of the plate and P is the pressure applied at the plate. For a compound membrane composed of two different materials, as shown in figure 2, the equivalent flexural rigidity, D_{eq}, can be calculated using [18]

$$D_{\text{eq}} = \frac{EE_1((l_{m1} - C)^3 + C^3)}{3} + \frac{EE_2((l_{m2} + l_{m1} - C)^3 - (l_{m1} - C)^3)}{3} \tag{2}$$

where

$$EE_1 = \frac{E_1}{1 - \sigma_1^2} \tag{3}$$

$$EE_2 = \frac{E_2}{1 - \sigma_2^2} \tag{4}$$

$$C = \frac{EE_1 l_{m1}^2 + EE_2\left[\left(l_{m1} + l_{m2}\right)^2 - l_{m1}^2\right]}{2\left(EE_1 l_{m1} + EE_2 l_{m2}\right)} \tag{5}$$

and where E, σ, ρ and l_m represent the Young modulus, Poisson's ratio, density and thickness of the material, respectively. Also indices 1 and 2 refer to *materials* 1 and 2, respectively, as shown in figure 2.

We have used this in-house software package to find the values of collapse voltage and resonant frequency of

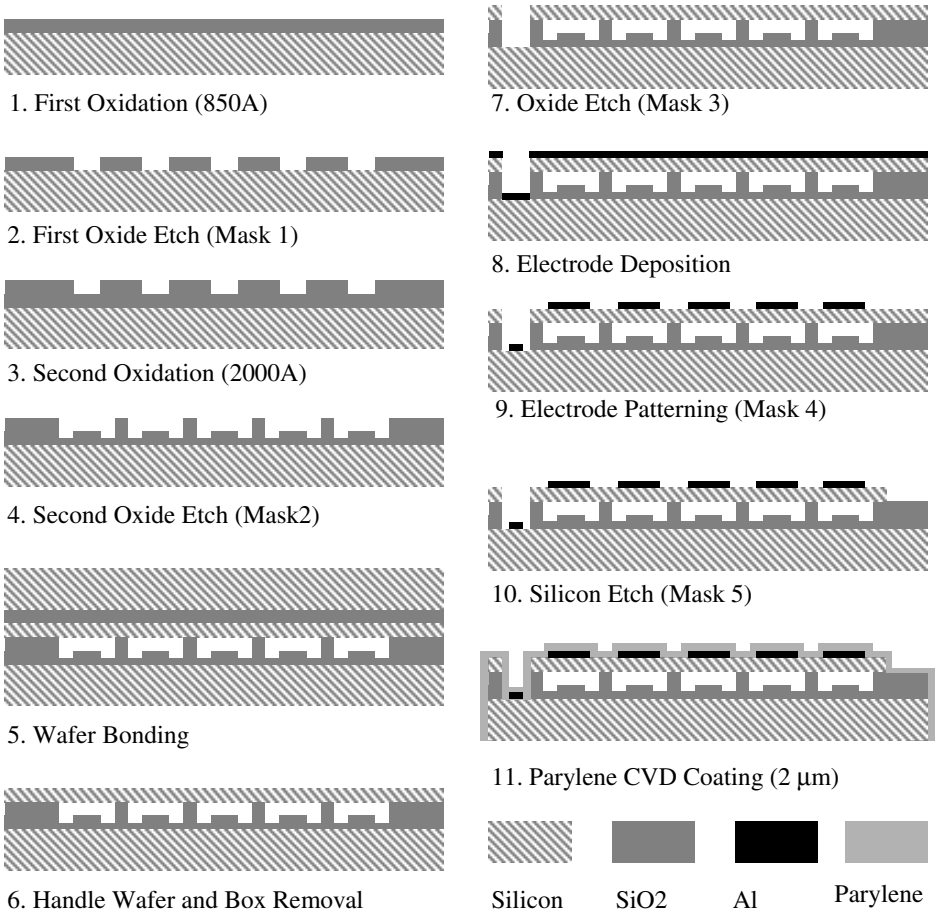

Figure 3. CMUT device fabrication diagram using a SOI wafer bonding process.

the device, before and after coating. The collapse voltage of a CMUT structure cannot be expressed as a closed-form formula and the software uses the proposed algorithm in [17] to calculate it. The lowest resonant frequency of the membrane in air, however, can be expressed as [19]

$$f_0 = \frac{1.6259}{a^2\sqrt{l_{m,\mathrm{eq}}}}\sqrt{\frac{D_{\mathrm{eq}}}{\rho_{\mathrm{eq}}}} \tag{6}$$

for a circular membrane of radius a, and

$$f_0 = \frac{3.5608}{W^2\sqrt{l_{m,\mathrm{eq}}}}\sqrt{\frac{D_{\mathrm{eq}}}{\rho_{\mathrm{eq}}}} \tag{7}$$

for a rectangular membrane of width W. In these formulae, $l_{m,\mathrm{eq}}$ and ρ_{eq} are the equivalent thickness and density of the compound membrane, respectively, and can be calculated as follows:

$$\rho_{\mathrm{eq}} = \frac{l_{m1}\rho_1 + l_{m2}\rho_2}{l_{m1} + l_{m1}} \tag{8}$$

$$l_{m,\mathrm{eq}} = l_{m1} + l_{m1}. \tag{9}$$

Note that for calculations before coating l_{m2} is set to zero.

3. Fabrication

Two different techniques for fabricating CMUT have been reported previously [20, 21]. The wafer bonding technique was used in this study, with an additional passivation layer deposition in step 11 (figure 3). A number of CMUT cell geometries are included in the mask layout. A 60 nm high cavity is etched in a highly conductive silicon wafer using both a buffered oxide etch (BOE) and a dry plasma etch. A silicon-on-insulator (SOI) wafer is then wafer bonded on top of the etched wafer using fusion bonding. The handle wafer is removed using wet etching in a hot tetramethylammonium hydroxide (TMAH) solution. The buried oxide layer is then removed by BOE, leaving a 2 μm membrane covering the cavities. Silicon membranes are separated by a dry plasma etch step. Then aluminum is deposited and ground and hot electrodes defined on the membrane and the silicon substrate, respectively. The devices are then separated from the wafer by dicing, and wire bonded to a printed circuit board. After wire bonding, the parylene is coated by vapor deposition polymerization (VDP) using a PDS 2010 Labcoater 2 (Cookson Electronics, Indianapolis, IN) to a final thickness of 2 $\pm$ 0.5 μm [22]. Figure 4 shows various views of the finished devices. The CMUT elements are 100 μm wide and 2 mm long.

While parylene is a relatively hard material, PDMS is soft. The softer PDMS provides good transcutaneous contact without the use of an ultrasonic gel layer. By coating CMUTs with PDMS, further insight can be gained into the coating effects on device performance. PDMS was spin coated to a thickness of 5 μm. The spin coating process did not allow for

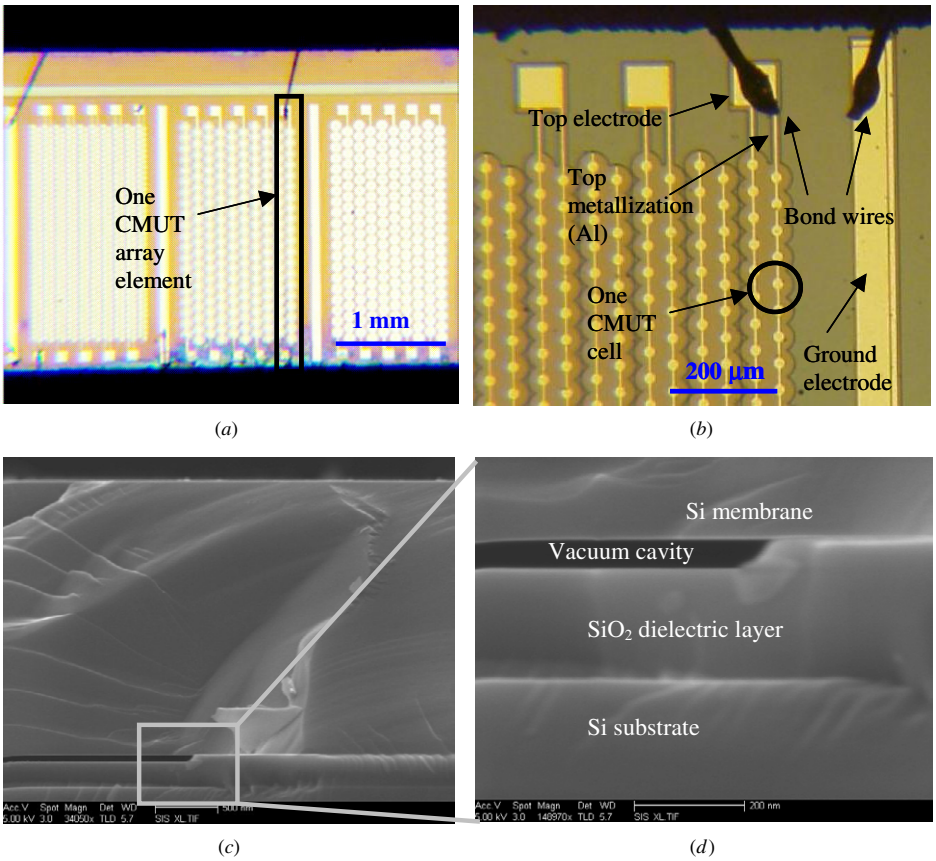

(*a*) (*b*) (*c*) (*d*)

Figure 4. Device pictures of (*a*) three different CMUT arrays, (*b*) a close-up of one array showing bond wires to both the top and bottom electrodes, (*c*) SEM cross-sectional view of a CMUT cell without coatings and (*d*) zoom in of (*c*) showing the membrane, cavity and dielectric layers.

coating of the bond wires. Therefore for the current PDMS coated devices, testing was completed in air only and no tests were performed underwater.

4. Device characterization

All the characterizations were carried out in the conventional mode. Throughout the operation in this mode, CMUT membranes are never in contact with the insulation layer covering the bottom electrode [23]. Coated and uncoated CMUTs were first characterized in air. A network analyzer (Model 8751, Hewlett-Packard Company, Palo Alto, CA) and a dc voltage supply (PS310, Stanford Research Systems, Sunnyvale, CA) were used to measure electrical input impedance of the array elements in air at different dc bias conditions. From the electrical input impedance measurements, the resonant frequency was determined as the frequency at which the real part of the impedance is maximal. The collapse voltage is defined as the voltage at which the electrostatic force between the membrane and the substrate overcomes the mechanical restoring force of the membrane, and the membrane contacts the bottom of the vacuum cavity. In the electrical input impedance measurements, the collapse voltage is determined by the abrupt change of the resonant frequency. The resonant frequencies and collapse voltages are summarized in table 2.

By coating the CMUT membranes with parylene, the collapse voltage increases due to the increased stiffness of the membranes. At the same time, the resonant frequency decreases. This is because the effects of the added mass overcome those of the added membrane stiffness. The measured values are compared with the analytical predictions based on the theory explained in section 2. Good agreement between theory and experimental results are obtained for resonant frequencies. The differences in the calculated and measured collapse voltages are likely due to the trapped electric charges in the dielectric layers of the CMUTs. In a CMUT with 48 μm circular cells, the real part of the input impedance shows a minimal value when the device is biased at about 25 V dc as opposed to 0 V dc, indicating a measurement offset of about 25 V. Similar charging effects were also observed in devices with other geometries. A method to prevent the charging effects in CMUTs has been reported in [24].

PDMS coating has a minimal effect on the membrane stiffness and the collapse voltage because it is a soft material. Due to the uncertainty and non-uniformity of the PDMS layer thickness as a result of spin coating on a die level, the predicted and measured resonant frequencies show certain differences. However, the general trends between the theory and measurement agree.

Figure 5 shows the real part of electrical input impedance for three similar CMUT devices with 48 μm circular cells:

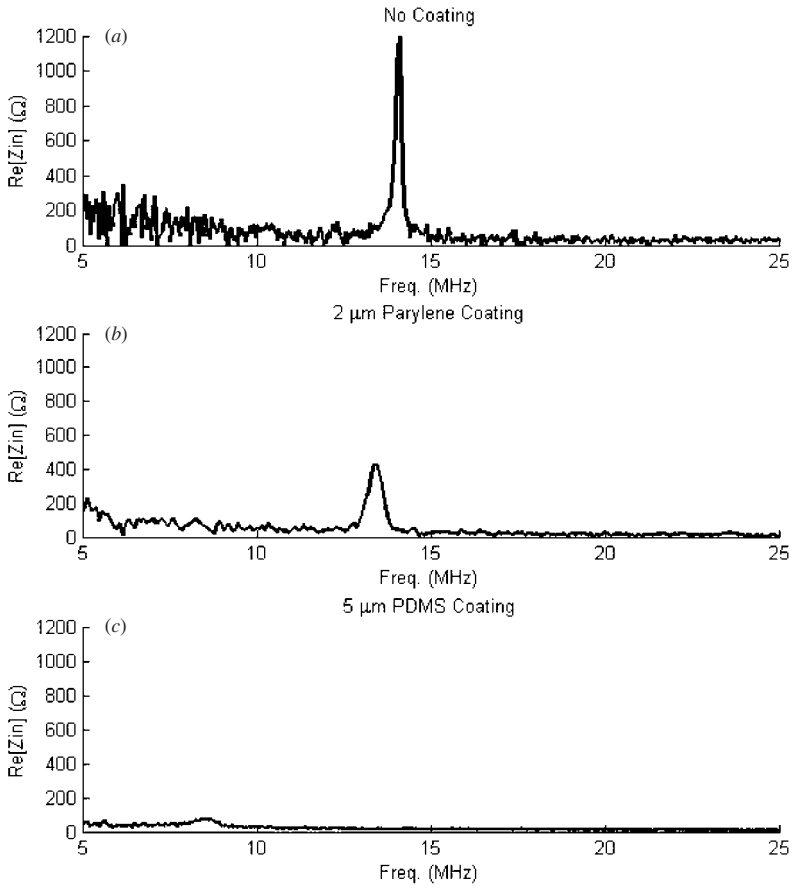

Figure 5. Effects of parylene and PDMS coatings on the real part of the input impedance of a device with 48 μm diameter circular membranes. (*a*) The peak amplitude is ∼1200 Ω (*b*) the peak amplitude decreases to ∼480 Ω and (*c*) the peak amplitude decreases to ∼100 Ω.

Table 2. Summary of test results in air on coated and uncoated CMUTs.

Coating material	CMUT Cell	Predicted resonant frequency (MHz)	Measured resonant frequency (MHz)	Predicted collapse voltage (V)	Measured collapse voltage (V)
No coating	31 μm diameter circle	31.9	30.7 (100 V dc bias)	88	132
	48 μm diameter circle	13.7	14.1 (40 V dc bias)	35	57
	27 μm wide rectangle	23.6	22.1 (70 V dc bias)	65	100
2 μm Parylene	31 μm diameter circle	28.5	28.5 (100 V dc bias)	98	144
	48 μm diameter circle	12.2	13.4 (40 V dc bias)	62	62
	27 μm wide rectangle	21.1	20.8 (70 V dc bias)	72	108
5 μm PDMS	31 μm diameter circle	22.3	27.4 (100 V dc bias)	88	138
	48 μm diameter circle	9.6	8.5 (40 V dc bias)	35	64
	27 μm wide rectangle	16.5	21.2 (70 V dc bias)	65	97

(a) uncoated, (b) coated with 2-μm parylene and (c) coated with 5 μm PDMS. As seen in this figure, a small amount of coating may significantly dampen the resonance in air due to the high loss in the coating material. In fact, as we can see in figure 6, the PDMS coated device has significantly more energy coupled to neighboring elements. However, the operation of the devices in water is different. The membrane motion is damped in the presence of water, and the coating layer should only increase the total stiffness of the membrane. Since the coating layer is thin (a fraction of acoustic wavelength), when operated in water the absorption of ultrasound should be minimal in the coating layer in the direction perpendicular to the membrane.

The membrane displacements and acoustic crosstalk in air were measured using a laser vibrometer (Polytec Inc., Tustin, CA). The CMUT arrays under comparison were of the same dimension (31 μm diameter circular cells) and were biased at the same voltage of 40 V. The ac excitation was a 20-cycle sinusoidal wave at the resonant frequency of the CMUT, with a peak-to-peak voltage of 10 V. One element was excited for each array, followed by a cell-by-cell scan to detect the maximum displacement of the active and inactive cells. The peak membrane displacement in air for the active cells decreased by 18% and 7% with the parylene and PDMS devices, respectively. In air, a slight increase in element-to-element crosstalk was seen for parylene coated devices and

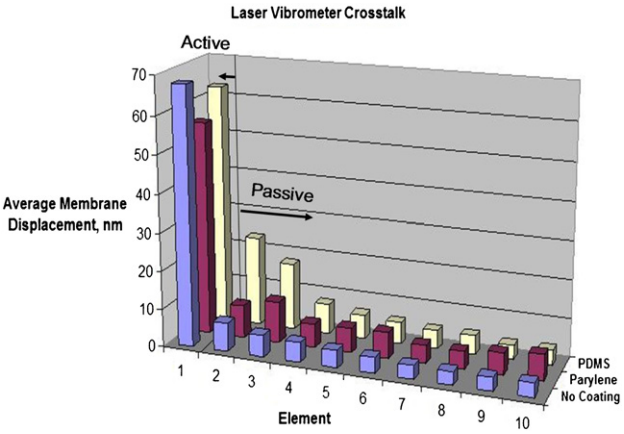

Figure 6. Crosstalk measurement results using a Polytec laser vibrometer.

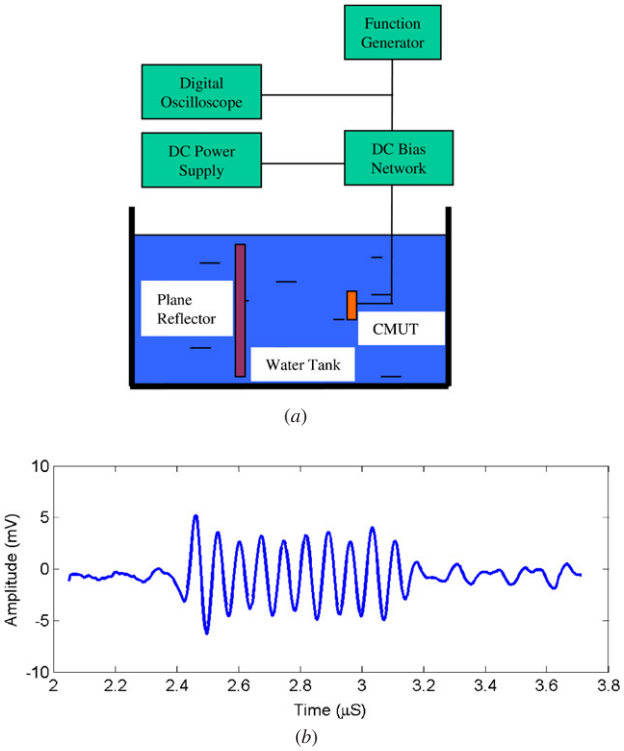

Figure 7. (*a*) Schematic of experimental setup for pulse-echo measurement. (*b*) Received echo signal in water.

a significant increase for devices with PDMS, as shown in figure 6.

Parylene coated devices were characterized in water. In one experiment, pulse-echo was performed in deionized water (DI water) to verify successful operation in an aqueous and corrosive medium. DI water is also known to corrode aluminum electrodes [25, 26]. Moreover, water breaks down when subjected to high electric field [27]. Figure 7(*a*) shows the pulse-echo experimental setup. An aluminum reflector was placed near the transducer surface. The device (31 μm cell diameter) was excited with a 10 V_{pp}, 10-burst, 14 MHz, sinusoidal ac voltage superimposed on a 70 V dc bias voltage. No leakage current was observed after applying the voltages. The CMUT transmitted a pulse and received the echo in a time

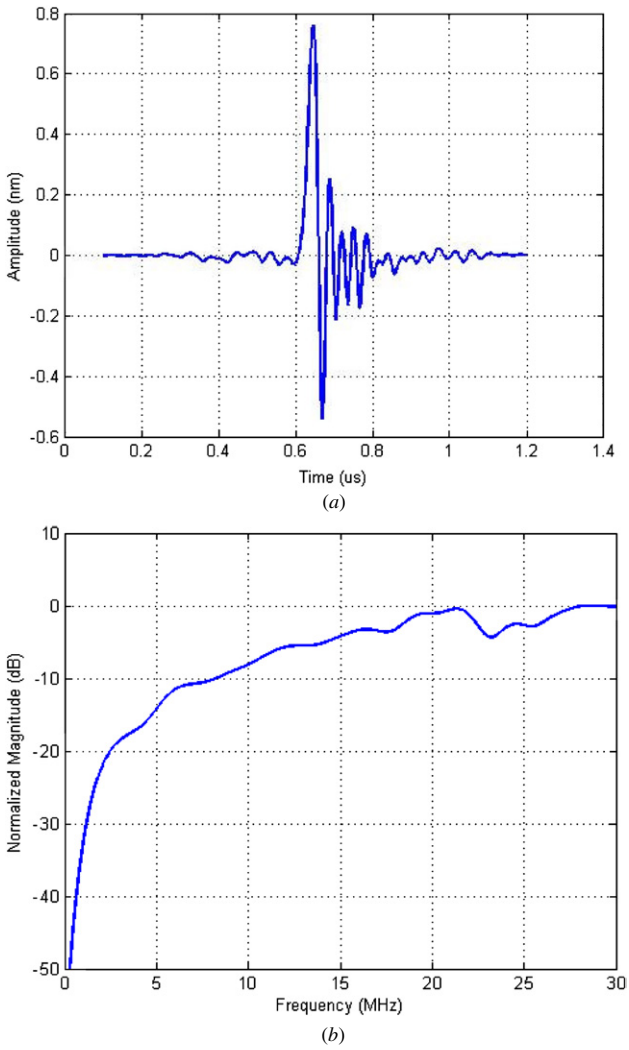

Figure 8. (*a*) Membrane center displacement in water measured with a laser vibrometer. (*b*) Corresponding velocity spectrum.

of 2.4 μs. The received signal is shown in figure 7(*b*). A similar test setup was also used to verify device performance when in contact with MediGel, a material acoustically similar to living tissue. The CMUT was excited by a pulse signal and the echo was received after 3.2 μs. No dc leakage current was observed.

In another experiment in water, the membrane displacement of a parylene-coated CMUT (25 μm cell diameter) was measured with the laser vibrometer. This device was biased at 130 V dc, and excited with a 10 ns, 16 V_{pp} ac pulse. Figure 8(*a*) shows the measured displacement at the center of the membrane in time domain. Figure 8(*b*) shows the corresponding velocity spectrum up to 30 MHz, which is the cutoff frequency of the laser vibrometer.

The degradation of parylene in tap water was also measured to assess coated device reliability. Full details of the pH value and ion contents of the tap water used in this experiment can be found in [28]. A CMUT device with parylene coatings of 2 $\pm$ 0.5 μm was tested while completely immersed in tap water. Passive immersion did not affect electrical isolation for a period of 14 days. A similar device was also tested with 1 kHz repetition rate pulse

excitation during immersion and remained electrically isolated and operational for over 48 h.

Additional testing of parylene coatings was performed on different micromachined structures conformally coated with 0.93 μm of parylene. A cantilever structure with boron doped piezoresistive region was biased as part of a full Wheatstone bridge with 10 V_{pp}. When the structure, piezoresistor, and interconnects were immersed in tap water, failure occurred around 100 h. An identical device was submersed in a 0.1 M phosphate buffered solution and failure was recorded after 1.5 h. Additional testing of actuated and passive devices coated with parylene in corrosive environments is necessary to determine the optimal coating thickness and expected lifetime for a given operating environment. A possible cause for the failure might be the delamination of the parylene layer. Investigations on adhesion promotion layers are planned to prolong the lifetime of the coating.

5. Conclusion

The parylene coating offered the necessary isolation and biocompatibility for CMUTs to be used in an aqueous and corrosive environment. The observed lifetimes of parylene coated devices may be sufficient for long-term use against skin. However, more evaluation is necessary for *in vivo* imaging in tissues and blood.

The results of testing PDMS coated devices in air are not enough for full reliability assessment. Spin coating of PDMS did not protect the bond wires, and the immersion tests were not performed. CMUTs with electrical through-wafer interconnects will facilitate the study of the effects of PDMS coating on device performance in immersion.

The change in resonant frequency and collapse voltage due to coating can be overcome with appropriate compensation in the dimensions of future device designs. Good agreement between the simulation and test results shows that the in-house analytical software package can be used to guide the design of CMUTs with coatings.

Thicker coating layers and multi-layer coatings are currently being researched. The acoustic characteristics of more coated CMUTs, especially in immersion, will be investigated. Electrical through-wafer interconnects will be incorporated with the next generation devices. Front-end electronic circuits will be integrated with these CMUTs. Ultimately, the feasibility of imaging pulsatile flow in the abdominal aorta of small organisms, such as neonatal mice will be studied using these devices.

Acknowledgments

The authors would like to thank Dr Ellis Meng at the University of Southern California for her time and help with parylene coating, and Dr Gokhan Percin for his help with the plate equations. This work was made possible with the help and support of Dr Richard Bland and was motivated by the lack of imaging systems for small animal models. We would also like to thank Alvin Barlian and Amy Lee for their support and hard work. This research was supported by seed funding from the Center for Integrated Systems. Work was performed in part at the Stanford Nanofabrication Facility (a member of the National Nanotechnology Infrastructure Network), which is supported by the National Science Foundation under grant ECS-9731293, its lab members and the industrial members of the Stanford Center for Integrated Systems.

References

[1] Eisenberg A 2004 An ultrasound that navigates every nook and cranny *New York Times* (15 January)

[2] Johnson J, Oralkan O, Demirci U, Ergun S, Karaman M and Khuri-Yakub P 2002 Medical imaging using capacitive micromachined ultrasonic transducer arrays *Ultrasonics* **40** 471–6

[3] Oralkan O, Ergun A S, Johnson J A, Karaman M, Demirci U, Kaviani K, Lee T H and Khuri-Yakub B T 2002 Capacitive micromachined ultrasonic transducers: next-generation arrays for acoustic imaging *IEEE Trans. Ultrason. Ferroelectr. Freq. Control* **49** 1596–610

[4] Yeh D T, Oralkan O, Wygant I O, O'Donnell M and Khuri-Yakub B T 2006 3D ultrasound imaging using a forward-looking CMUT ring array for intravascular/intracardiac applications *IEEE Trans. Ultrason. Ferroelectr. Freq. Control* **53** 1202–11

[5] Specialty Coating Systems 2006 http://www.scscoatings.com/

[6] Armani D *et al* 1999 Re-configurable fluid circuits by PDMS elastomer micromachining *MEMS (Orlando, FL)* pp 222–7

[7] Harder T A, Yao T-J, He Q, Shih C-Y and Tai Y-C 2002 Residual stress in thin-film parylene-c *IEEE Int. Conf. on Micro Electro Mechanical Systems (MEMS) (Las Vegas, NV)* pp 435–8

[8] 1999 *Polymer Data Handbook* (New York: Oxford University Press)

[9] Foster F S 2000 Transducer materials and probe construction *Ultrasound Med. Biol.* **26** S2–5

[10] Hadimioglu B and Khuri-Yakub B T 1990 Polymer films as acoustic matching layers *IEEE Ultrasonics Symp. (Honolulu, HI)* pp 1337–40

[11] Seyed-Bolorforosh M S 1995 Novel integrated impedance matching layer *IEEE Trans. Ultrason. Ferroelectr. Freq. Control* **42** 809–11

[12] Voskerician G, Shive M S, Shawgo R S, Von Recum H, Anderson J M, Cima M J and Langer R 2003 Biocompatibility and biofouling of MEMS drug delivery devices *Biomaterials* **24** 1959–67

[13] Liger M, Rodger D C and Tai Y-C 2003 Robust parylene-to-silicon mechanical anchoring *IEEE Int. Conf. on Micro Electro Mechanical Systems (MEMS) (Kyoto)* pp 602–5

[14] Weisenberg B A and Mooradian D L 2002 Hemocompatibility of materials used in microelectromechanical systems: platelet adhesion and morphology in vitro *J. Biomed. Mater. Res.* **60** 283–91

[15] Barlian A A, Narain R, Li J T, Quance C E, Ho A C, Mukundan V and Pruitt B L 2006 Piezoresistive MEMS underwater shear stress sensors *IEEE Int. Conf. on Micro Electro Mechanical Systems (MEMS) (Istanbul, Turkey)* pp 626–9

[16] Xu Y and Tai Y-C 2003 Selective deposition of parylene-c for underwater shear-stress sensors *12th Int. Conf. on Transducers, Solid-State Sensors, Actuators and Microsystems (Boston)* pp 1307–10

[17] Nikoozadeh A, Bayram B, Yaralioglu G G and Khuri-Yakub B T 2004 Analytical calculation of collapse voltage of CMUT membrane *IEEE Ultrasonics Symp. (Montréal, QC, Canada)* pp 256–9

[18] Certon D, Teston F and Patat F 2005 A finite difference model for CMUT devices *IEEE Trans. Ultrason. Ferroelectr. Freq. Control* **52** 2199–210

[19] Peake W H and Thurston E G 1954 The lowest resonant frequency of a water-loaded circular plate *J. Acoust. Soc. Am.* **26** 166–8

[20] Haller M and Khuri-Yakub B T 1994 A surface micromachined electrostatic ultrasonic air transducer *IEEE Ultrasonics Symp. (Cannes, France)* pp 1241–4
[21] Yongli H, Ergun A S, Haeggstrom E, Badi M H and Khuri-Yakub B T 2003 Fabricating capacitive micromachined ultrasonic transducers with wafer-bonding technology *J. Microelectromech. Syst.* **12** 128–37
[22] Meng E and Tai Y 2005 Parylene etching techniques for microfluidics and biomems *IEEE Int. Conf. on Micro Electro Mechanical Systems (MEMS)* pp 568–71
[23] Bayram B, Yaralioglu G G, Kupnik M, Ergun A S, Oralkan O, Nikoozadeh A and Khuri-Yakub B T 2005 Dynamic analysis of capacitive micromachined ultrasonic transducers *IEEE Trans. Ultrason. Ferroelectr. Freq. Control* **52** 2270–5
[24] Yongli H, Haeggstrom E O, Xuefeng Zhuang E O, Ergun A S and Khuri-Yakub B T 2005 A solution to the charging problems in capacitive micromachined ultrasonic transducers *IEEE Trans. Ultrason. Ferroelectr. Freq. Control* **52** 578–80
[25] Berzins A, Evans J V and Lowson R T 1977 Aluminum corrosion studies: II. Corrosion rates in water *Aust. J. Chem.* **30** 721–31
[26] Vos R, Rotondaro A, Mertens P W, Meuris M and Heyns M 1997 A novel environmentally-friendly corrosion-free post-stripping rinsing procedure after solvent strip *VLSI Technol.* pp 37–8
[27] Toriyama Y and Shinohara U 1937 Electric breakdown field intensity of water and aqueous solutions *Phys. Rev.* **51** 680
[28] Stanford University Utilities Division 2005 http://facilities.stanford.edu/environment/Web2005CCR.pdf